JOURNAL OF AIRCRAFT
Vol. 37, No. 3, May–June 2000

Closed-Loop Control of Forebody Flow Asymmetry

John E. Bernhardt* and David R. Williams†
Fluid Dynamics Research Center, Illinois Institute of Technology, Chicago, Illinois 60616

A closed-loop digital control system was designed for a tangent-ogive forebody model to control the flow asymmetry during an unsteady pitching maneuver using suction ports located at the tip of the forebody. A feedback control system was also developed to control the coning angle ϕ of a coning motion model. The performance of both linear and nonlinear control laws was studied and evaluated. The controllers designed for the pitching forebody model were most effective for angles of attack less than 50 deg. For $\alpha > 50$ deg, the controllers had difficulty in maintaining the pressure coefficient near the desired value of zero, which corresponded to a symmetric vortex configuration. The control system designed for the coning motion model enabled the model to perform a variety of different maneuvers. Experiments demonstrated the ability of the system to control the coning angle of the model, its rotation rate, and the direction of rotation.

Nomenclature

C_p = pressure coefficient, $\Delta p/(\frac{1}{2}\rho U_0^2)$
D = maximum diameter of the forebody model
k_d = derivative gain of the proportional integral derivative (PID) control law
k_i = integral gain of the PID control law
k_p = proportional gain of the PID control law
R_{vp} = correlation coefficient between the angular velocity and the pressure coefficient
Re = Reynolds number, $U_0 D/\nu$
U_0 = freestream velocity
Δp = pressure difference measured by the two Kulite transducers

Introduction

IN the latter part of the 1970s and early 1980s, the tactical advantages of supermaneuverability for fighter aircraft increased interest in poststall maneuverability. Studies by Herbst[1] have shown that the ability to maneuver at high angles of attack can provide a very effective tactical advantage for close-in aerial combat situations. The Herbst maneuver performed by the X-31 aircraft involves high-angle-of-attack aerodynamics and a velocity vector roll (coning motion) at an angle of attack near 90 deg. Ericsson and Beyers[2] discuss the high alpha aerodynamics associated with the Herbst maneuver. Utilizing this maneuver, the X-31 aircraft can reverse its flight direction with a significantly smaller radius of curvature than for a conventional turn. The high degree of maneuverability demonstrated by the X-31 was primarily achieved by using thrust vectoring and advanced digital control schemes.

To perform maneuvers in the poststall flight regime, the X-31 had to overcome several constraints that limited the capabilities of conventional aircraft at high angles of attack. One important issue that had to be addressed was the development and management of asymmetric vortices on the forebody section of the aircraft. For many years, it has been known that the asymmetric vortices can produce large side forces on slender bodies of revolution. The vortex system induces an asymmetric pressure distribution on the surface of the forebody. Intergration of the pressure distribution over the surface yields a net side force. The direction of the side force (yaw left or right) is not predictable. The side force begins to develop on the forebody at approximately $\alpha = 30$ deg and continues to be significant for angles of attack up to 60 deg.

The large side forces and yawing moments produced by the asymmetric forebody vortices can affect the yaw control characteristics of an aircraft and limit the maneuverability. At high angles of attack, the forebody vortices interact with the wing and vertical tail surfaces. These interactions can lead to roll oscillations of the aircraft called wing rock. Furthermore, the large side forces created by the asymmetric vortices can generate a torque resulting in the rotation of the vehicle about its center of gravity, which is known as coning motion. The coning motion of the body has been studied extensively by Tobak et al.,[3] Schiff and Tobak,[4] Ericsson and Reding,[5] and Yoshinaga et al.[6]

Small geometric imperfections in the forebody tip appear to be responsible for the overall vortex asymmetry. Experiments by Lamont,[7] Bridges and Hornung,[8] Dexter and Hunt,[9] Zilliac et al.,[10] and Moskovitz[11] all showed that the side force varied with roll angle, indicating a correlation between the vortex configuration and the position of the geometric asymmetry. Additional support for the microasymmetry concept has been provided by the numerical experiments of Degani.[12] Degani found that it was necessary to introduce a small geometric disturbance at the tip to force an asymmetirc flow. Furthermore, Bernhardt and Williams[13] studied the response of the forebody flow asymmetry at $\alpha = 45$ and 55 deg by using suction and blowing through small ports located at the tip of the forebody model.

One mechanism that has been proposed to explain the development of the vortex asymmetry is based on a spatial instability concept.[12,14,15] The small geometric imperfections at the tip of the forebody produce an initial flow asymmetry. This initial tip asymmetry is amplified by the flow along the axis of the forebody. The development of the vortex asymmetry in the axial direction is then due to the amplification of the initial flow asymmetry by a spatial instability in the forebody wake.

Early attempts at forebody vortex control were primarily directed at alleviating the side force and associated yawing moment by forcing the flow into a symmetric vortex configuration. One of the simplest and least expensive approaches is to use strakes located at the tip of the forebody. Nose strakes have been successfully applied on a wide range of aircraft from the X-15 to the X-31. The sharp edges of the strakes force the flow separation lines to be symmetric. The forebody vortices then form in a symmetric configuration and remain relatively symmetric behind the aircraft. Malcolm[16] reports that strakes are most effective for $30 < \alpha < 60$ deg, and can reduce yawing moments by as much as a factor of three. The disadvantages of nose strakes are increased drag and loss of vortex-induced lift on the forebody. Other passive control methods include helical trips, transition strips, and increasing nose bluntness. Roos and Magness[17] were able to maintain nearly symmetric flow for $0 < \alpha < 60$ deg on a tangent-ogive cylinder by blunting the nose radius to 20% of the

Received 14 March 1999; revision received 27 December 1999; accepted for publication 29 December 1999.

*Postdoctoral Research Assistant, Department of Materials, Mechanical, and Aerospace Engineering, Member AIAA.
†Professor, Department of Materials, Mechanical, and Aerospace Engineering, Associate Fellow AIAA.

base radius. For all passive control devices, the goal is to reduce side forces and yawing moments by forcing a symmetric flow state. Consequently, passive control devices cannot take full advantage of the forebody asymmetry to enhance maneuverability.

Active control methods focus on the ability to manipulate both the magnitude and direction of the side force. Active control requires the capacity to change the forebody vortex system between a yaw-left and yaw-right configuration. Active control schemes offer the potential to improve maneuverability by exploiting the side forces and yawing moments generated by the asymmetric vortices. For example, yawing moments could be increased during turns at high angles of attack for the purpose of decreasing the turning radius. A number of different active control actuators have been used to modify the forebody vortex asymmetry. Jet blowing experiments have been conducted on a generic fighter aircraft by Malcolm and Ng.[18] Additional experiments using jet blowing have been carried out on a scaled F-15E by Roos,[19] whereas Eidson and Mosbarger[20] utilized a scaled F-16 aircraft. Bernhardt and Williams[13] and Williams and Bernhardt[21] have investigated the effects of unsteady bleed, suction, and blowing on forebody vortex asymmetry.

Experiments have shown that active control of the vortex asymmetry in the tip region can be accomplished with very low power levels compared to the side force thrust power on the body. Control with gains, between the actuator input and side force thrust power output, on the order of 10^8 have been measured in low Reynolds number experiments.[13] Low forcing amplitudes and input power levels are possible due to the spatial amplification of disturbances in the forebody wake.

The active control techniques mentioned earlier essentially operate in an open-loop mode. A controlled disturbance is placed into the flow near the tip of the forebody and the response of the vortices to the control is measured in terms of the side force or yawing moment. However, this approach does not provide a method by which a particular value of the side force can be selected and maintained at a given angle of attack or during an unsteady maneuver. The reason is that open-loop control methods do not employ feedback from the forebody vortices. The next logical step is to incorporate the active control actuators into a complete closed-loop control system that employs feedback from the forebody vortices. Closed-loop control systems are needed to take full advantage of these active control techniques. The control techniques require proper timing with the motion of the aircraft and the behavior of the flowfield. In addition, using a feedback control system offers the possibility of an expanded flight envelope to even higher angles of attack. Buffington and Adams[22] have numerically investigated this using a closed-loop controller on a modified Variable-Stability Inflight Simulator Test Aircraft (VISTA) F-16 aircraft and were able to show that an active control system would have satisfactory maneuverability through $\alpha = 35$ deg.

Experiments conducted for this investigation will demonstrate the feasibility of using closed-loop control systems to manipulate the forebody vortices at high angles of attack. Feedback control systems will be developed for both pitching forebody and coning motion models. Steady suction is used for the experiments to control the development of the asymmetric forebody vortices. The forcing is applied through small control ports located at the tip of the forebody model. The performance of linear and nonlinear control laws will be studied and evaluated.

Experimental Configuration

The experiments were conducted in a low-speed, open-return wind tunnel at the Fluid Dynamics Research Center of the Illinois Institute of Technology. The test section of the wind tunnel was 1.83 m long by 0.41 m wide by 0.61 m high (72 in. by 16 in. by 24 in). Honeycomb and screens placed ahead of the nine-to-one contraction reduced the freestream turbulence level in the test section to less than 0.25%.

Pitching Forebody Model

The forebody model designed for the pitching experiments is shown in Fig. 1 with auxiliary views of the cone. The length of the model was 34.29 cm (13.5 in.) and the diameter was 2.54 cm (1.0 in.). These dimensions resulted in a fineness ratio of 13.5. The model also featured a tangent-ogive cone with an L/D ratio of 3.5. The control ports consisted of small holes of diameter 1.6 mm (0.0625 in.) drilled into each side of the cone tip. The control ports were located at ± 135 deg from the forward stagnation line. Each control port was connected to a separate internal tube, so that each port could be independently activated. A pair of needle valves controlled the amount of suction applied at the tip of the cone. Hoke brass needle valves connected the control port tubes to the vacuum system. A flexible shaft adapter connected each needle valve to a Bodine stepping motor. The position of the stepper motor was controlled using digital output from a 486-type personal computer. The level of suction applied through a particular control port was adjusted by rotating the shaft of the stepper motor from one angular position to another. This rotary motion caused the coupled needle valve to open or close.

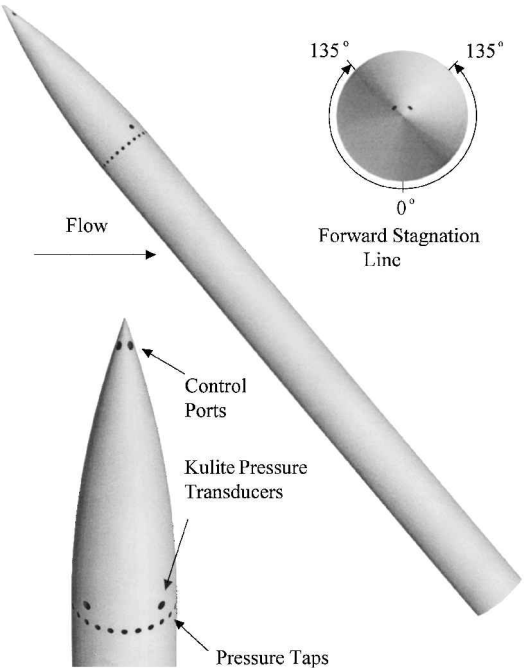

Fig. 1 Illustration of the tangent-ogive forebody model.

Two Kulite pressure transducers were mounted on the surface of the model at ± 135 deg from the forward stagnation line. The pressure transducers were located at an axial distance of $Z/D = 3.14$. The main purpose of the pressure transducers was to detect changes in the configuration of the forebody vortices. The data from the pressure transducers provided an instantaneous measure of the surface pressure at two spatial locations. For this case, the pressure coefficient C_p was defined as the difference in the pressures measured by the transducers divided by the dynamic pressure. The experimental accuracy of the C_p measurements was estimated to be ± 0.04. The pressure taps shown in Fig. 1 were not used for the experiments.

The pitching forebody model was supported by a mounting sting inserted through the floor of the test section. The wind-tunnel mounting sting was connected by a series of linkages to a PMI Motion Technologies dc motor. The positioning system enabled the model to be pitched through a selected angle-of-attack range. A 486-type personal computer controlled the trajectory of the model. The stand design incorporated a rotating mechanism that allowed for model alignment with the freestream flow.

Coning Motion Model

The coning motion model had a tangent-ogive nose cone with an L/D ratio of 3.5. This cone was interchangeable with the pitching forebody model. The cylinder portion of the coning motion model had a length of 17.94 cm (7.06 in.) and a diameter of 2.54 cm (1.0 in.). The overall fineness ratio for the model was 10.6. Figure 2 shows a side view of the coning motion model. A splitter plate attached

to the model made the flow symmetric on the lower section of the cylinder. As a result, the side force acting on the model was mainly produced by the asymmetric tip vortices. A piece of modeling clay fixed to the end of the cylinder statically balanced the model. Instrumentation for the coning motion model consisted of an optical encoder and a slip ring. A steel shaft attached to the mounting sting was coupled to the encoder by a piece of flexible plastic tubing. Digital data from a MicroKinetics series incremental encoder was used to calculate the angular position and velocity of the model. The encoder operated in quadrature mode and had a resolution of 0.045 deg. Because of the rotary motion of the model, a slip ring was required to provide electrical connections for the pressure transducers. Selected for this purpose was a Maurey Instruments slip ring assembly.

A mounting sting made from a length of thin-walled steel tubing supported the coning motion model during the wind-tunnel experiments. A pair of set screws fastened the model to the mounting sting and made it possible to adjust the angle of attack. The mounting sting was supported at one end by two ball bearings. Two aluminum rings were used to connect the external control port tubes to the internal tubes that ran through the mounting sting. The rings were inserted between the bearings in an alternating sequence. A sealed bearing was employed between the rings to minimize leakage. Model alignment with the freestream flow was accomplished by an azimuthal rotation of the base plate.

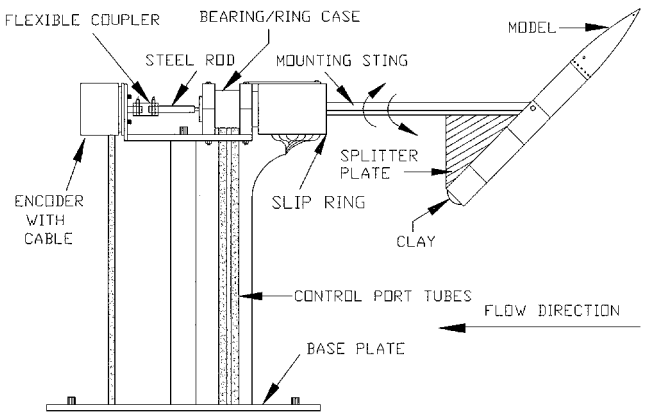

Fig. 2 Side view of the coning motion model.

Closed-Loop Control Systems and Algorithms

Pitching Forebody Model

A digital feedback control system with output sampling was developed for the pitching forebody model. The control system was designed to manipulate the flow asymmetry during an unsteady pitching maneuver. Specifically, the experiments focused on the ability of the control system to maintain a particular flow state throughout the entire angle-of-attack range. The controlled output variable was the pressure coefficient C_p. A block diagram representation of the control system is shown in Fig. 3. The controller was digitally implemented using a 486-type personal computer. The command input C_p represented the desired flow state of the vortex system during the pitching maneuver, that is, yaw left, symmetric, or yaw right. The computer calculated the current value of the pressure coefficient, which corresponded to the existing flow state. The controller used the error to determine the actuating signal. The control signal was sent by digital output to the actuator. The actuator consisted of the two needle valve/stepper motor devices. In this case, the system to be controlled was the pair of asymmetric tip vortices. The two Kulite pressure transducers mounted on the surface of the model acted as the feedback sensors.

A digital proportional integral derivative (PID) control law was developed for the pitching forebody model. The control law gains were selected using a trial-and-error procedure. For this procedure, the forebody model underwent an unsteady pitching maneuver. The unsteady maneuver consisted of a pitch-up motion where the angle of attack varied from 20 to 70 deg. The angle-of-attack history had the form of a cosine function with a pitch rate $\dot{\alpha}$ of 5 deg/s. The control system had a sampling rate of 45 Hz and the Reynolds number was 6×10^4. The desired value of C_p was selected to be zero, which corresponded to the symmetric vortex configuration. Because the pressure coefficient had only one value at low angles of attack and could not be manipulated, the control law was not activated until α reached 25 deg. The optimum gains were found to be $k_p = 18.0$, $k_i = 27.5$, and $k_d = 0.006$.

Another interesting approach to the control of the asymmetric tip vortices involved a controller that used a neural network in parallel with a Proportional Derivative (PD) control law as depicted in

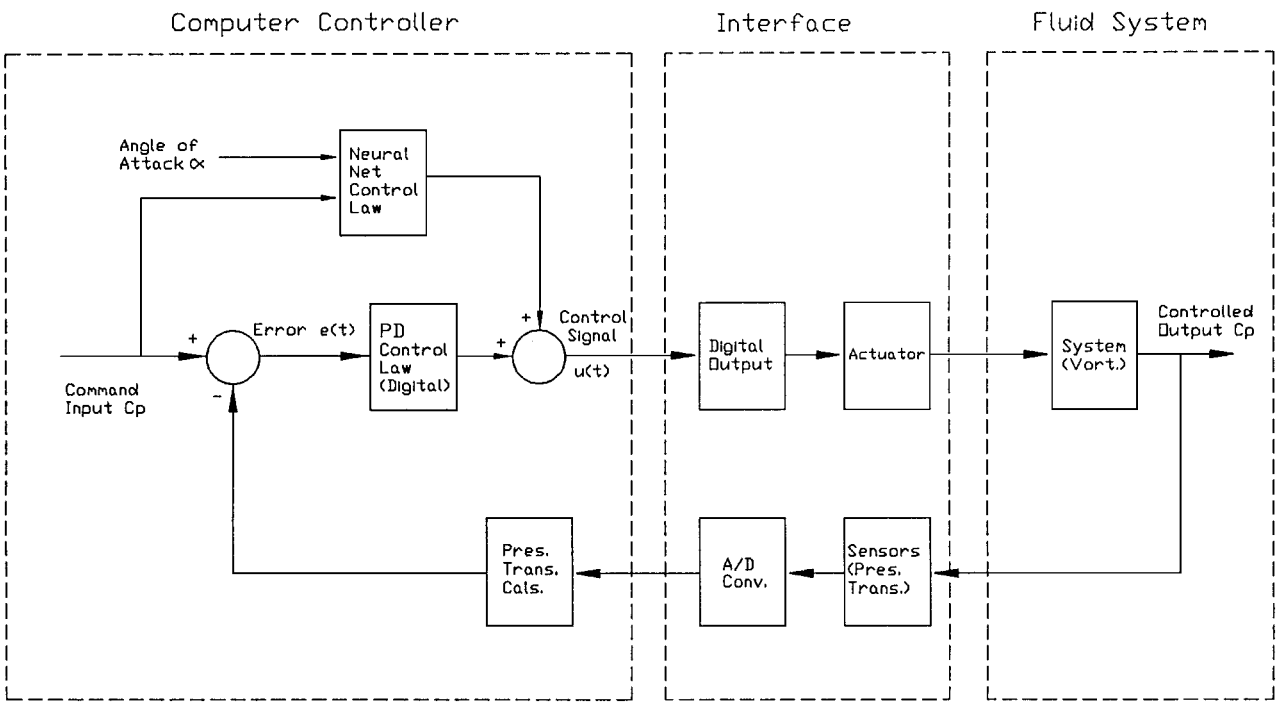

Fig. 3 Block diagram of the feedback control system for the pitching forebody model with a neural network-PD controller.

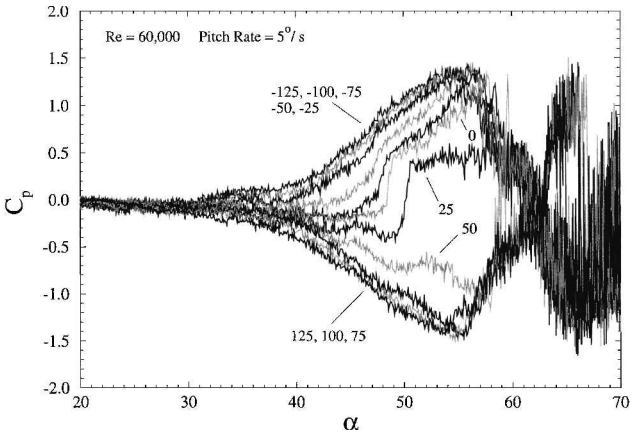

Fig. 4 Control map for the pitching forebody model.

Fig. 3. The controller configuration used feedforward compensation realized as a nonlinear neural network. The neural network control law, however, operated in an open-loop mode. To close the loop, a PD control law was added. The control signal was determined by a contribution from both of the control laws.

The training and testing data sets for the backpropagation neural network were derived from the control envelope. This control envelope is displayed in Fig. 4. Each curve in Fig. 4 shows the response of the vortex system for a single pitch-up motion with a fixed actuator position. The response of the vortex system was measured in terms of the pressure coefficient C_p. The pressure coefficient values used for the two data sets were limited to angles of attack from 40 to 56 deg. The training set contained pressure data from the control curves in 2-deg increments starting at $\alpha = 40$ deg. Pressure coefficient values taken from the control map at $\alpha = 41, 45, 49$, and 53 deg composed the testing data set. The angle-of-attack range was selected based on several considerations. Previous experiments with the PID control law demonstrated that it was capable of maintaining the pressure coefficient near zero for $\alpha < 40$ deg. Furthermore, the control map indicated that for angles of attack approaching 55 deg the vortices became locked in to one of two possible configurations. Essentially, only two values of the pressure coefficient were attainable, and intermediate states could not be achieved.

The neural network model represented the inverse of the system described by the control envelope. The inputs for the neural network were the desired value of the pressure coefficient and the angle of attack. The angle of attack was included as an input because it was an important parameter in determining the state of the system. The output for the neural network was the actuator position. The commercial software package NeuralWorks Professional II/Plus performed the necessary training and testing of the networks. The neural network selected for the controller had two hidden layers with five processing elements in each layer. This network architecture was chosen because it performed well on both the training and testing data sets. The gains of the PD control law were set using a trial-and-error approach as described earlier. The sampling rate for the control system was 60 Hz, and the control law was not activated until α reached 25 deg. The optimum gains were found to be $k_p = 30.0$ and $k_d = 0.031$.

Coning Motion Model

The closed-loop control scheme that was used with the coning motion model utilizes a proportional integral (PI) control law with velocity feedback compensation. For velocity feedback compensation, the derivative of the system output was added to the control law output. The control signal was then a combination of these two components. The controlled output variable was the coning angle ϕ. A coning angle of $\phi = 0$ deg corresponded to a vertical orientation of the model with the tip pointed toward the test section ceiling. Positive values of the coning angle occurred for a clockwise rotation of the model as viewed along its axis, whereas negative values occurred for a counterclockwise rotation. An optical encoder coupled to the mounting sting provided feedback of the coning angle to the controller. The coning rate of the model was computed from the position information for velocity feedback purposes.

Two different maneuvers were selected to demonstrate the capabilities of the control system. Both of the maneuvers were performed at a Reynolds number of 5.5×10^4 with the angle of attack fixed at 55 deg. The control objective of the first maneuver was to position the model at a coning angle of -105 deg starting from the steady coning rate for the unforced asymmetric case. For the second maneuver, the model was required to move from a coning angle of -105 to -15 deg and then return to the initial coning angle of -105 deg. A step input was applied to the control system for the purpose of moving the model between the two coning angles. Tuning of the controller gains was accomplished by a trial-and-error procedure with a sampling rate of 20 Hz. The experiments indicated that the integral component of the controller did not improve the performance of the control system, and so the integral gain was set to zero for both maneuvers. The controller gains were found to be, for maneuver 1: $\phi = -105$ deg, $k_p = 0.040$, $k_d = 0.030$; and for maneuver 2: $-105 \rightarrow -15$ deg, $k_p = 0.040$, $k_d = 0.100$; $-15 \rightarrow -105$ deg, $k_p = 0.040$, $k_d = 0.040$.

Results

Control Map for the Pitching Forebody Model

The control map represents the set of all attainable states that the control system can achieve during the unsteady pitching maneuver. For the results presented in this section, the region of control expressed in terms of C_p vs α defines the control map as shown in Fig. 4. Each curve is labeled with an actuator setting measured in steps of the stepper motor. Actuator positions range from -125 to $+125$ in increments of 25. The curve labeled with a zero represents the unforced asymmetric case, that is, the case where no control was applied. A positive value of the actuator position designates suction applied through one of the control ports, whereas a negative value denotes forcing through the control port on the opposite side. The actuator setting was fixed for each curve, so that the amount of suction at the tip remained constant during the pitch-up motion.

The control map clearly shows several features that emphasize the important fluid physics of the flowfield that would be generic to any flight vehicle. For angles of attack from 20 to 30 deg, all of the curves are coincident. The value of the pressure coefficient is approximately zero, which corresponds to the symmetric vortex configuration. Bernhardt and Williams[13,23] have shown experimentally that a symmetric pressure distribution, that is, a pressure coefficient of approximately zero, signifies a symmetric vortex configuration at least from the forebody tip to the pressure measurement location. The result for low angles of attack is perhaps not surprising because the tip vortices remain attached to the body and may not be fully formed. As the angle of attack is increased beyond 30 deg, the range of C_p values that can be achieved also increases. For instance, the pressure coefficient range at $\alpha = 50$ deg is near maximum and is certainly much greater than at 30 deg. In addition, the curves have spread apart indicating an increased sensitivity of C_p to the applied control.

As the angle of attack approaches 55 deg, the pressure coefficient values converge to one of two possible curves. The convergence of the pressure coefficient indicates that only two vortex configurations are possible. This type of vortex behavior is referred to as a two-state condition. Note that the two-state condition shown by the control map may not exist at higher Reynolds numbers. As demonstrated by Bernhardt and Williams,[24] the two-state behavior of the vortex system changes to a continuous behavior as the Reynolds number is increased. Therefore, control authority may be extended to higher angles of attack at higher Reynolds numbers. As the actuator position increases, the pressure coefficient curves tend to reach the limiting curves. The limiting curves correspond to actuator positions of ± 125 in Fig. 4. The limiting curves define the outer envelope of the control region. The control system must operate within the region defined by the limiting curves.

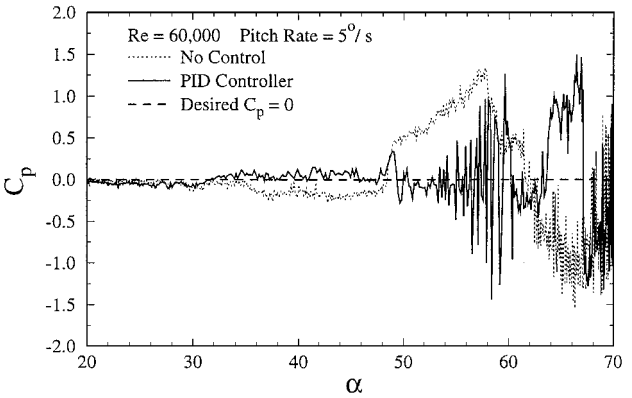

a) $\dot{\alpha} = 5$ deg/s

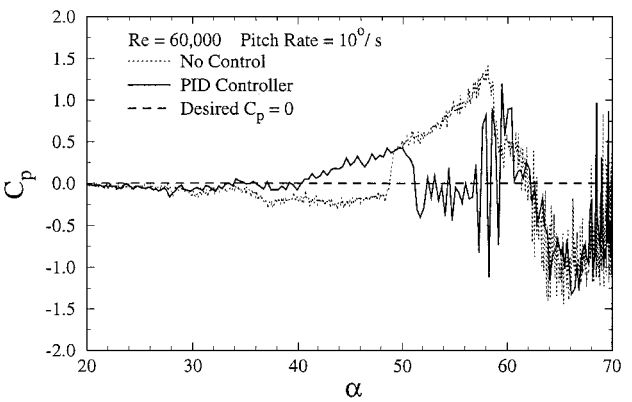

b) $\dot{\alpha} = 10$ deg/s

Fig. 5 Comparison of the unforced asymmetric and controlled cases for the tangent-ogive forebody model during pitch-up maneuvers using a PID control law.

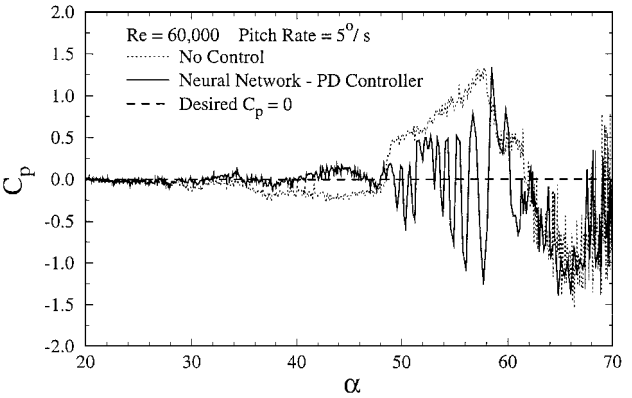

a) $\dot{\alpha} = 5$ deg/s

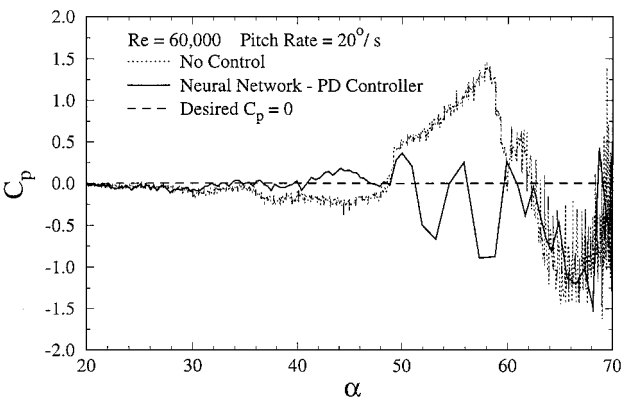

b) $\dot{\alpha} = 20$ deg/s

Fig. 6 Comparison of the unforced asymmetric and controlled cases for the tangent-ogive forebody model during pitch-up maneuvers using a neural network-PD control law.

Flow Asymmetry Control for the Pitching Forebody Model

A comparison between the unforced asymmetric case (dotted line) and the controlled case (solid line) is shown in Fig. 5a for the pitching forebody model with $\dot{\alpha} = 5$ deg/s and $Re = 6 \times 10^4$. It is clearly seen from Fig. 5a that the PID controller was able to modify the pressure coefficient during the pitching maneuver. In addition, the PID controller was able to maintain C_p close to the desired value of zero for angles of attack up to 49 deg. At $\alpha = 49$ deg, a sudden jump in C_p occurred from 0.05 to 0.34. The controller applied a corrective action to drive the pressure coefficient toward zero, but eventually an oscillation developed. The amplitude of the oscillation increased with angle of attack and the controller could no longer maintain the pressure coefficient near zero. Figure 5b presents the results for the same PID controller where the pitch rate has been increased to 10 deg/s. It can be seen from Fig. 5b that the controller had more difficulty keeping C_p near zero, especially in the range $40 < \alpha < 50$ deg.

The second controller designed for the pitching forebody model was a nonlinear controller consisting of a neural network in combination with a PD control law. Comparisons between the unforced asymmetric and controlled cases are shown in Fig. 6 for a Reynolds number of 6×10^4 and pitch rates of 5 and 20 deg/s. By comparing the two cases in Fig. 6a, it is apparent that the controller was able to modify the pressure coefficient and maintain C_p close to the desired value of zero up to $\alpha = 49$ deg. For angles of attack greater than 49 deg, an oscillation in C_p occurred and the controller was no longer able to maintain the pressure coefficient near zero. Figure 6b shows a similar result for the higher pitch rate of 20 deg/s. The controller was again effective up to $\alpha = 49$ deg, at which point oscillations in the pressure coefficient appeared.

The control systems used to manipulate the forebody flow asymmetry include a time delay between the actuator and the pressure transducers. It takes a finite amount of time for the forcing to travel from the valve to the control port. In addition, a finite time is required for the control applied at the tip to convect along the model axis and reach the location of the pressure transducers.[13] These two times added together comprise the time delay t_d, which was found to be approximately 0.015 s for $\alpha = 40$ deg and $Re = 3 \times 10^4$. The time delay can be normalized by the convective timescale L/U_0, where L is the length of the forebody model. The normalized time delay was calculated to be $\tau_d = 0.78$. This normalized time delay is a factor of three shorter than the value measured by Lanser and Meyn.[25]

Coning Motion Control

The time history of the coning angle for the first maneuver is displayed in Fig. 7a for $\alpha = 55$ deg and $Re = 5.5 \times 10^4$. The dotted line drawn in Fig. 7a represents the desired value of the coning angle $\phi = -105$ deg. The results for the coning rate and the pressure coefficient are shown in Figs. 7b and 7c, respectively. The value of the pressure coefficient at the start of the maneuver was -0.78. The negative value of C_p indicates that the vortices were initially arranged in a yaw-left configuration. Consequently, the model rotated in the counterclockwise direction at a coning rate of -1161 deg/s. This coning rate corresponds to a rotational frequency of 3.2 Hz.

As the maneuver progressed, the forcing amplitude increased at the tip, causing the pressure coefficient to increase and reach a value of zero. The model decelerated due to the decrease in the torque produced by the tip vortices. At $\dot{\phi} = 0$, the model stopped rotating and a change in the direction of motion occurred. The coning angle at this point was -152 deg, and the model had rotated through 3.1 revolutions. For positive values of C_p, the yaw-right configuration of the vortices generated a clockwise torque on the model. As ϕ approached -105 deg, both the pressure coefficient and the coning rate oscillated about values of zero. The time required to perform the maneuver was 2.9 s.

An analysis of the correlation between the angular velocity of the model and the pressure coefficient is shown in Fig. 8. The time delay

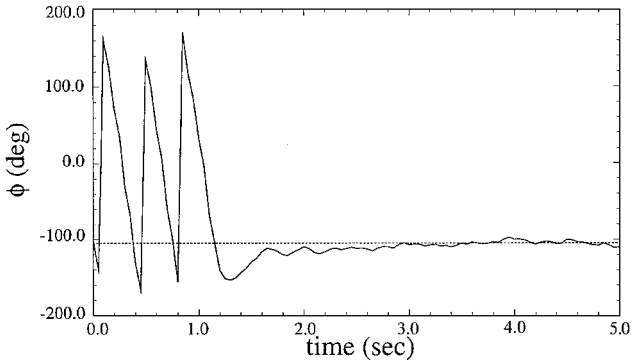

a) Coning angle

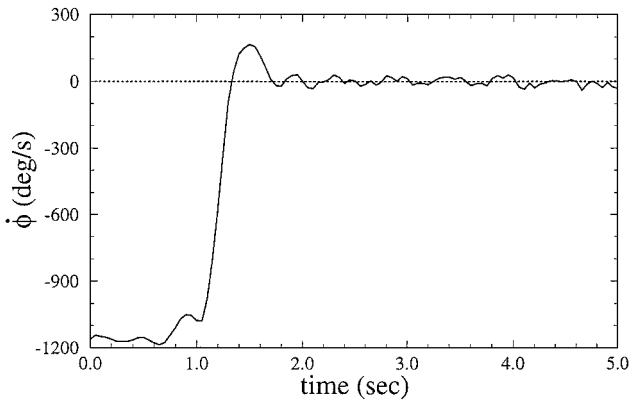

b) Coning rate

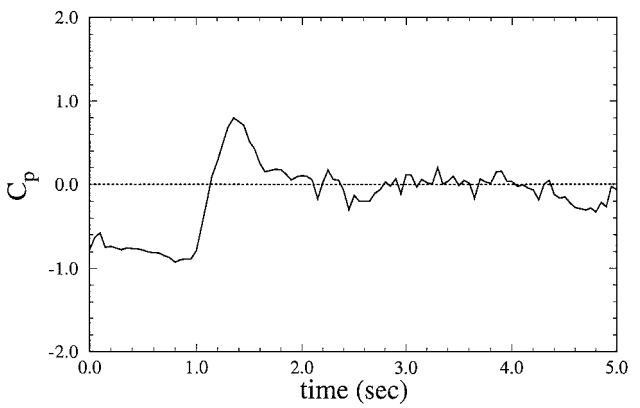

c) Pressure coefficient

Fig. 7 Time history for the first maneuver to position the coning motion model at $\phi = -105$ deg.

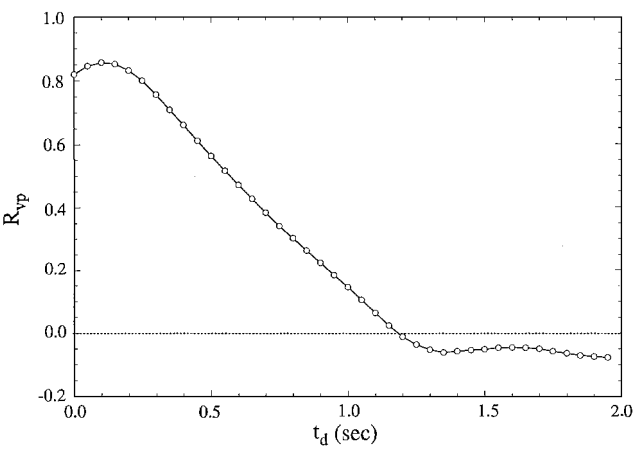

Fig. 8 Correlation between the angular velocity of the coning motion model and the pressure coefficient.

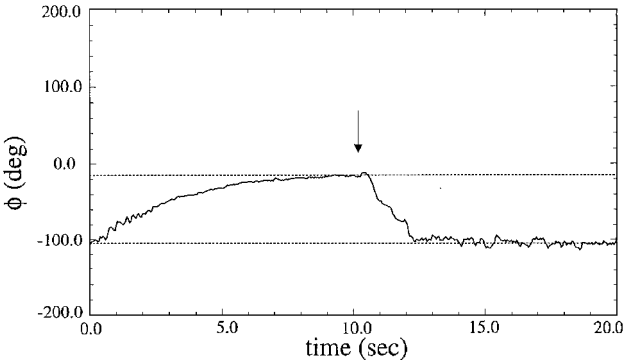

a) Coning angle

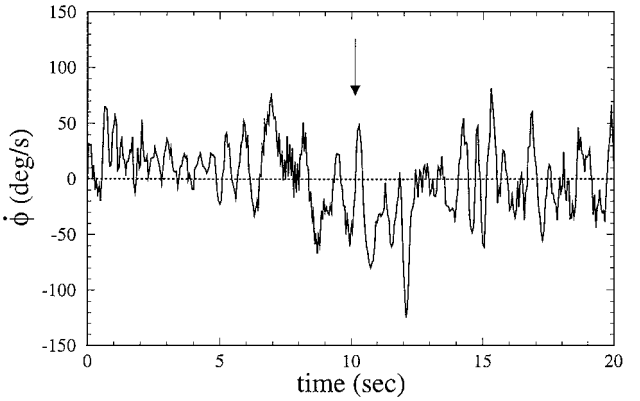

b) Coning rate

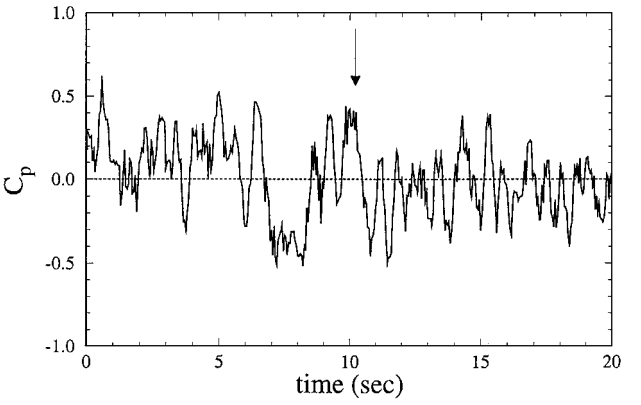

c) Pressure coefficient

Fig. 9 Time history for the second maneuver to move the coning motion model between $\phi = -105$ deg and -15 deg.

t_d is measured relative to the angular velocity. For a time delay of 0.1 s, the correlation coefficient reaches a maximum value of 0.86. For larger time delays, the correlation coefficient steadily decreases and eventually levels off at a value of -0.08. This result reveals that the angular velocity lags the pressure coefficient by approximately 0.1 s. The time delay can be normalized by the convective time scale L/U_0, and was calculated to be $\tau_d = 12.1$.

The second maneuver consisted of moving the model between coning angles of -105 and -15 deg. Figure 9a shows the time history of the coning angle for this maneuver where the arrow marks the beginning of the return motion. The model was moved from a coning angle of -105 to -15 deg in approximately 9.2 s. Oscillations in the coning angle developed at the start of the motion but were damped by the control system. The yaw-right configuration of the vortex system rotated the model in the clockwise direction as can be seen in Figs. 9b and 9c. The model returned to the initial coning angle of $\phi = -105$ deg in a time of 3.9 s. The shorter time period for the return motion is clearly illustrated in Fig. 9a. Negative values for both the coning rate and the pressure coefficient can be seen in Fig. 9b and 9c during the return motion of the model.

The counterclockwise rotation of the model was a result of the yaw-left vortex configuration as indicated by the negative values of the pressure coefficient.

Discussion

Pitching Forebody Model Control System

It is clear from the experiments that both the PID and neural network–PD controllers are capable of manipulating the pressure coefficient during an unsteady pitching maneuver. The controllers are most effective for angles of attack less than 50 deg. For $\alpha > 50$ deg, the controllers have difficulty in maintaining the pressure coefficient at the desired value. Oscillations in the pressure coefficient occur for all the controllers.

The ineffectiveness of the controllers for angles of attack greater than 50 deg can be explained by considering the timescales of the control system. The two important timescales are the response time of the actuator and the time constant associated with the vortex dynamics. The actuator response time was estimated to be 0.025 s, which included a time delay of 0.015 s plus an additional 0.010 s for the movement of the stepper motor. The time constant associated with the vortex dynamics was approximately 0.023 s for $\alpha > 50$ deg. Therefore, the time constant of the vortex dynamics was comparable to the actuator response time. The actuator response was not fast enough to keep pace with the changes in the vortex system and the corresponding variations of the pressure coefficient. The positioning of the actuator is especially critical at these angles of attack due to the increased sensitivity of the pressure coefficient to the applied control. Thus, it is the actuator response time that limits the performance of the control system.

The actuator response time includes a fixed time delay between the control valve and the pressure transducers as reported earlier. Note that a pure time delay always has a destabilizing effect on a control system and can limit the overall response time. Thus, it is not surprising that the actuator response time limits the control system performance because it includes the fixed time delay. The destabilizing effect of the time delay appears as an oscillation of the pressure coefficient. The amplitude of the oscillation increases as the two-state behavior of the vortex system is reached for angles of attack approaching 55 deg. The increase in the amplitude of the oscillation may indicate the start of a limit cycle behavior for the control system.

For angles of attack less than 50 deg, the PID controller is more sensitive to changes in the pitch rate than the neural network–PD controller. A comparison of the controllers at $\dot{\alpha} = 5$ deg/s shows that the linear PID control algorithm is as effective as the nonlinear neural network approach. As the pitch rate is increased to 10 deg/s, the PID controller encounters difficulty in maintaining the pressure coefficient near zero. The performance of the neural network controller, however, is not significantly influenced by an increase of the pitch rate to 20 deg/s. This characteristic of the controller can be attributed to the neural network portion of the control law. The majority of the control burden is placed on the neural network. The PD component of the controller only adds a small correction to the control signal. The neural network was trained on the experimental data from the control map shown in Fig. 4. The effect of pitch rate on the control map is negligible for an increase of $\dot{\alpha}$ from 5 to 20 deg/s. Therefore, pitch rate effects do not significantly change the performance of the controller. In contrast, the gains for the PID controller depend on the pitch rate. The pitch rate strongly influences the controller performance in this case.

Coning Motion Model Control System

The results presented demonstrate the capabilities of the position control system designed for the coning motion model. The system has the ability to control the coning angle of the model, the coning rate, and the direction of rotation for a variety of different maneuvers. As illustrated by Fig. 8, the angular velocity of the model is correlated with the pressure coefficient. The correlation is expected because a splitter plate was attached to the lower half of the model. The flow around the lower half of the model was symmetric and produced zero net torque. The tip vortices on the upper half of the model generated the necessary torque for the rotation. The correlation coefficient reaches a maximum value for a time delay between the two signals of 0.1 s. This result confirms that the angular velocity lags the pressure coefficient. As explained earlier, it takes a finite amount of time for the flow downstream to respond to changes in the initial flow conditions at the tip. A fixed amount of time must elapse before the side force develops on the model. Furthermore, the coning motion model has inertia. Because of the inertia, changes in the angular velocity of the model occur over a finite period of time.

Position control of the coning motion model was accomplished for coning angles in the range from -15 to -105 deg. For coning angles outside this range, the control system encountered difficulty in positioning the model. It appears from this behavior of the control system that the tip vortices could be interacting with the side walls of the wind tunnel. The tip vortices have corresponding image vortices located outside of the test section. As the model approaches the side walls, the image vortices interact with the tip vortices. This interaction influences the motion of the model and affects its controllability. The presence of the side wall effect introduces a dependence of the system behavior on the coning angle ϕ. This dependence on ϕ is reflected in the gains selected for the controllers. For instance, the set of controller gains used to move the model from $\phi = -105$ to -15 deg is different from that for the return motion back to the initial coning angle of -105 deg.

The oscillations of the pressure coefficient can be attributed to the unsteadiness of the flowfield. As C_p approaches zero, the separation points of the forebody vortices move closer to the tip, which allows the vortex shedding to occur over a larger portion of the model. The enhanced vortex shedding on the lower portion of the model induces unsteadiness in the forebody vortices. A similar type of flow unsteadiness has been documented for the forebody model by Bernhardt.[26] Numerical computations by Degani and Schiff[27] demonstrate the unsteadiness of the forebody vortices for both symmetric and slightly asymmetric configurations. The oscillations produce corresponding fluctuations in the angular position and velocity of the model. Once again, the response of the actuator is not fast enough to damp out the fluctuations.

The control systems that have been discussed in this paper focus on the pressure coefficient measured by the Kulite transducers. The pressure coefficient indicates the state of the vortex system, but is only a local measurement in space. Variables that measure the flow asymmetry on a global scale must also be considered. These important variables include the side and normal forces as well as the yawing and pitching moments. Force and moment measurements have been made by Bernhardt[26] for a round-tip tangent-ogive model at $\alpha = 40$ deg and $Re = 4 \times 10^4$. Bernhardt found a 17% decrease in the normal force and a 22% increase in the pitching moment referenced to the unforced asymmetric values. These minimum and maximum points occurred as the total side force and yawing moment passed through values of zero. The corresponding value of the pressure coefficient was -0.23, which indicated a slightly asymmetric arrangement of the forebody vortices. Therefore, forebody flow asymmetry control is more than just a matter of attempting to manipulate the vortex configuration to change the pressure coefficient or the side force. The effects of the control on the normal force and pitching moment must also be considered in the overall flight vehicle control scheme.

Conclusions

A closed-loop control system was designed for the tangent-ogive forebody model to control the flow asymmetry during an unsteady pitching maneuver. A feedback control system was also developed to control the position of the coning motion model. This control system enabled the coning motion model to perform a variety of different maneuvers. The performance of both linear and nonlinear control laws was studied and evaluated. The experimental results have demonstrated the feasibility of using a closed-loop control system to manipulate the forebody flow asymmetry. Thus, similar control systems can be used to manipulate the vortex configuration and the side force on a flight vehicle to enhance the maneuverability at angles of attack up to 55 deg.

The control map for the pitching forebody model shows interesting features that have important control implications. The control map clearly shows that for angles of attack between 20 and 30 deg, the pressure coefficient is fixed at a value of approximately zero. Consequently, at low angles of attack the vortex configuration and the side force cannot be controlled. As the angle of attack is increased, the pressure coefficient curves spread apart indicating an increased sensitivity to the applied control. This increased sensitivity requires a more precise setting of the actuator position.

The controllers designed for the pitching forebody model were most effective for angles of attack less than 50 deg. For $\alpha > 50$ deg, the controllers had difficulty in maintaining the pressure coefficient near the desired value of zero. The actuator response time limits the performance of the control systems mainly due to the time delay between the control valve and the pressure transducers. The slow actuator response time coupled with the increased sensitivity of the vortex system leads to the ineffectiveness of the controllers. In addition, a two-state behavior of the vortex system occurs as the angle of attack approaches 55 deg. The two-state behavior locks in the vortex configuration making it difficult for the controllers to maintain the pressure coefficient at the desired value.

The time delay is an important system property for both the pitching forebody and coning motion models. For example, a strong correlation exists between the pressure coefficient and the angular velocity of the coning motion model. The maximum value of the correlation coefficient occurs for a time lag of 0.1 s. The time lag is partly due to the time delay between the application of the control at the tip and the response of the flow downstream. It takes a finite amount of time for the side force to develop on the model. This time delay determines how rapidly the side force can be changed on a flight vehicle.

The model inertia provides the second important contribution to the time lag. Once the side force has developed, it takes a finite amount of time for the angular velocity to change due to the inertia of the model. This time delay determines how quickly the angular velocity can be changed on an actual flight vehicle. The time lag will place a limit on the overall response time of the control system.

The measurements acquired from the round-tip tangent-ogive model show a strong coupling between the lateral and longitudinal forces and moments. As the side force and yawing moment reach values of zero, the normal force decreases by 17% and the pitching moment increases by 22% relative to the unforced asymmetric case. These results imply that the control of forebody flow asymmetry is more than just an attempt to manipulate the vortex configuration to control the side force. Because of the large changes in the normal force and the pitching moment, the effects of the control on the longitudinal characteristics of the flight vehicle must be considered in the overall control scheme.

Acknowledgments

This investigation has been conducted with the support of the Air Force Office of Scientific Research under Contract F49620-93-1-0106 monitored by Daniel Fant, James McMichael, and Leonard Sakell. The assistance of Nabeel Tarabishy in developing the neural network controller is greatly appreciated. The authors would like to thank Jaime Arenas, Martin Fraske, and Alberto Quintanna for their contributions to the design and construction of the experimental models.

References

[1]Herbst, W. B., "Supermaneuverability," *Proceedings of the Workshop on Unsteady Separated Flow*, edited by M. S. Francis and M. W. Luttges, U.S. Air Force Academy, 1983, pp. 1–9.

[2]Ericsson, L. E., and Beyers, M. E., "Conceptual Fluid/Motion Coupling in the Herbst Supermaneuver," *Journal of Aircraft*, Vol. 34, No. 3, 1997, pp. 271–277.

[3]Tobak, M., Schiff, L. B., and Peterson, V. L., "Aerodynamics of Bodies of Revolution in Coning Motion," *AIAA Journal*, Vol. 7, No. 1, 1969, pp. 95–99.

[4]Schiff, L. B., and Tobak, M., "Results from a New Wind-Tunnel Apparatus for Studying Coning and Spinning Motions of Bodies of Revolution," *AIAA Journal*, Vol. 8, No. 11, 1970, pp. 1953–1957.

[5]Ericsson, L. E., and Reding, J. P., "Dynamics of Forebody Flow Separation and Associated Vortices," *Journal of Aircraft*, Vol. 22, No. 4, 1985, pp. 329–335.

[6]Yoshinaga, T., Tate, A., and Inoue, K., "Coning Motion of Slender Bodies at High Angles of Attack in Low Speed Flow," AIAA Paper 81-1899, Aug. 1981.

[7]Lamont, P. J., "Pressures Around an Inclined Ogive Cylinder with Laminar, Transitional, or Turbulent Separation," *AIAA Journal*, Vol. 20, No. 11, 1982, pp. 1492–1499.

[8]Bridges, D. H., and Hornung, H. G., "Elliptic Tip Effects on the Vortex Wake of an Axisymmetric Body at Incidence," *AIAA Journal*, Vol. 32, No. 7, 1994, pp. 1437–1445.

[9]Dexter, P. C., and Hunt, B. L., "Effects of Roll Angle on the Flow Over a Slender Body of Revolution at High Angles of Attack," AIAA Paper 81-0358, Jan. 1981.

[10]Zilliac, G., Degani, D., and Tobak, M., "Asymmetric Vortices on a Slender Body of Revolution," AIAA Paper 90-0388, Jan. 1990.

[11]Moskovitz, C. A., "An Experimental Investigation of the Physical Mechanisms Controlling the Asymmetric Flow Past Slender Bodies at Large Angles of Attack," Ph.D. Thesis, Dept. of Mechanical and Aerospace Engineering, North Carolina State Univ., Raleigh, NC, June 1989.

[12]Degani, D., "Numerical Investigation of the Origin of Vortex Asymmetry," AIAA Paper 90-0593, Jan. 1990.

[13]Bernhardt, J., and Williams, D., "Effect of Reynolds Number on Control of Forebody Asymmetry by Suction and Bleed," AIAA Paper 93-3265, July 1993.

[14]Degani, D., and Tobak, M., "Numerical Simulation of Upstream Disturbance on Flows Around a Slender Body," AIAA Paper 93-2956, July 1993.

[15]Degani, D., and Tobak, M., "Experimental Study of Controlled Tip Disturbance Effect on Flow Asymmetry," *Physics of Fluids A*, Vol. 4, No. 12, 1992, pp. 2825–2832.

[16]Malcolm, G. N., "Forebody Vortex Control—A Progress Review," AIAA Paper 93-3540, Aug. 1993.

[17]Roos, F. W., and Magness, C. L., "Bluntness and Blowing for Flowfield Asymmetry Control on Slender Forebodies," AIAA Paper 93-3409, Aug. 1993.

[18]Malcolm, G. N., and Ng, T. T., "Aerodynamic Control of Fighter Aircraft by Manipulation of Forebody Vortices," CP-497, AGARD Paper 15, Nov. 1991.

[19]Roos, F. W., "Microblowing for High-Angle-of-Attack Vortex Flow Control on a Fighter Aircraft," AIAA Paper 96-0543, Jan. 1996.

[20]Eidson, R. C., and Mosbarger, N. A., "Forebody Pneumatic Devices at Low Angles of Attack and Transonic Speed," AIAA Paper 97-0042, Jan. 1997.

[21]Williams, D., and Bernhardt, J., "Proportional Control of Asymmetric Forebody Vortices with the Unsteady Bleed Technique," AIAA Paper 90-1629, June 1990.

[22]Buffington, J. M., and Adams, R. J., "Nonlinear Vortex Flow Control for High Angle of Attack Maneuvering," *Control Engineering Practice*, Vol. 3, No. 5, 1995, pp. 631–642.

[23]Bernhardt, J., and Williams, D., "Proportional Control of Asymmetric Forebody Vortices," *AIAA Journal*, Vol. 36, No. 11, 1998, pp. 2087–2093.

[24]Bernhardt, J., and Williams, D., "The Effect of Reynolds Number on Vortex Asymmetry about Slender Bodies," *Physics of Fluids A*, Vol. 5, No. 2, 1993, pp. 291–293.

[25]Lanser, W. R., and Meyn, L. P., "Forebody Flow Control on a Full-Scale F/A-18 Aircraft," *Journal of Aircraft*, Vol. 31, No. 6, 1994, pp. 1365–1371.

[26]Bernhardt, J., "Closed-Loop Control of Forebody Flow Asymmetry," Ph.D. Thesis, Dept. of Mechanical and Aerospace Engineering, Illinois Inst. of Technology, Chicago, Il, May 1996.

[27]Degani, D., and Schiff, L., "Numerical Simulation of the Effect of Spatial Disturbances on Vortex Asymmetry," AIAA Paper 89-0340, Jan. 1989.